



HAL
open science

High-order X-FEM for image-based computations

Grégory Legrain, Nicolas Chevaugeon

► **To cite this version:**

Grégory Legrain, Nicolas Chevaugeon. High-order X-FEM for image-based computations. 6th EUROPEAN CONGRESS ON COMPUTATIONAL METHODS IN APPLIED SCIENCES AND ENGINEERING (ECCOMAS 2012), 2012, Vienna, Austria. hal-01008256

HAL Id: hal-01008256

<https://hal.science/hal-01008256>

Submitted on 16 Mar 2024

HAL is a multi-disciplinary open access archive for the deposit and dissemination of scientific research documents, whether they are published or not. The documents may come from teaching and research institutions in France or abroad, or from public or private research centers.

L'archive ouverte pluridisciplinaire **HAL**, est destinée au dépôt et à la diffusion de documents scientifiques de niveau recherche, publiés ou non, émanant des établissements d'enseignement et de recherche français ou étrangers, des laboratoires publics ou privés.

HIGH-ORDER X-FEM FOR IMAGE-BASED COMPUTATIONS

G. Legrain¹ and N. Chevaugeon¹

¹Lunam Université - Ecole Centrale Nantes, Université de Nantes - GeM Institute, UMR CNRS 6183
1, rue de la Noë, 44321 Nantes
e-mail: {gregory.legrain,nicolas.chevaugeon}@ec-nantes.fr

Keywords: X-FEM, Partition of Unity, High-order, Nitsche's method

Abstract. *In this contribution, a strategy is proposed for treating geometrically complex problems such as those encountered in image-based analysis. The use of the X-FEM allows the treatment of such applications without the need to mesh the geometry. However, the geometrical accuracy is still linked to the size of the finite element mesh because of the interpolation of the level-set. An approach is proposed for uncoupling geometrical description and approximation in this context. The strategy is based on a uniform coarse mesh that defines a high order approximation of the mechanical fields and an adapted mesh that defines the geometrical features by means of levelsets. The connection between the geometry and the approximation is obtained by sharing the quadtree trees of the two meshes. Numerical examples involving level-set based parts and image-based microstructures are presented.*

1 INTRODUCTION

Since the beginning of the development of finite elements, various approaches were proposed in order to try to uncouple geometry and approximation. In particular, the fictitious domain approach restricts the integration of the weak formulation to the solid part of the domain. This approach has been improved recently in the context of the Finite Cells approach [1] by the use of high order shape functions, and a sub-grid representation of the geometry. In the context of partition of unity methods, both X-FEM and GFEM were also considered for solving problems by means of an unfitted mesh. Both of these methods were considered in the context of (moderate) high-order approximations [2, 3, 4, 5, 6]. However, high-order methods require to master geometrical errors in order to ensure their convergence. Various schemes were proposed in order to represent the geometry in this case (pixelized integration [7], quasi-regional mapping for the integration cells [7], on the fly tetrahedrization [3]) Additional issues comes from the use of level-sets in the X-FEM. Indeed, the geometry is represented implicitly on the finite element mesh, which means that the geometrical representation depends on the finite element mesh. Thus, accurate geometry requires refined meshes close to the interfaces, and thus increase the computational cost of the approach [8]. Two possibilities can be considered:

1. Define a high-order level-set representation [9, 5]
2. Represent the level-set on a finer mesh [6]

2 UNCOUPLING GEOMETRY AND APPROXIMATION

The last approach is considered here. It is based on [6], but with the use of two meshes (see figure 1): a coarse one defining the approximation, and an adapted one (finer near the interfaces) for the geometry. The two meshes are built using a common octree database, which means that the geometrical mesh is nested into the approximation mesh. The link between the two meshes is obtained naturally thanks to the common octree database. It was shown in [6] that optimal convergence rates could be obtained in the case of free surfaces, but also that the ridge enrichment function (which has to be modified in this case) could not provide optimal rates. We propose here to use Nitsche's method in this case, with a discontinuous enrichment across the interface.

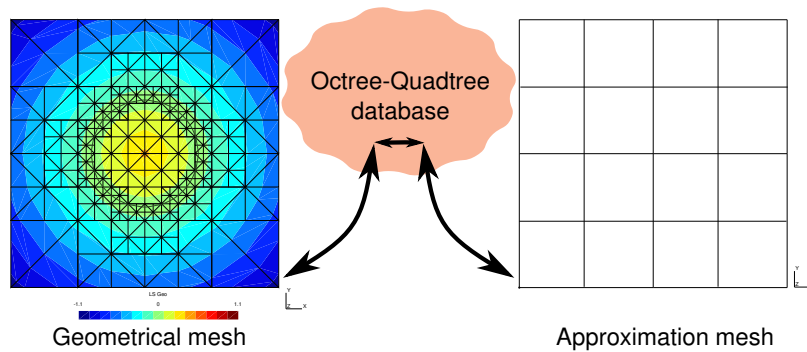


Figure 1: Principle of the proposed approach

In this case, the weak form of the problem is modified as follows:

$$a(\mathbf{u}, \mathbf{v}) - \int_{\Gamma} \{\underline{\underline{\sigma}} \cdot \mathbf{n}\} \llbracket \mathbf{v} \rrbracket d\Gamma - \int_{\Gamma} \{\delta \underline{\underline{\sigma}} \cdot \mathbf{n}\} \llbracket \mathbf{u} \rrbracket d\Gamma + \beta \int_{\Gamma} \llbracket \mathbf{u} \rrbracket \llbracket \mathbf{v} \rrbracket d\Gamma = l(\mathbf{v}) \quad (1)$$

where $a(\mathbf{u}, \mathbf{v})$ and $l(\mathbf{v})$ are respectively the classical linear and bilinear forms of a mechanical problem. $\{\bullet\}$ is the average operator and $[[\bullet]]$ is the jump operator. In this paper, $\{\bullet\}$ is defined as $1/2[\bullet(\mathbf{x}^+) + \bullet(\mathbf{x}^-)]$, and $[[\bullet]]$ as $1/2[\bullet(\mathbf{x}^+) - \bullet(\mathbf{x}^-)]$ where $\bullet(\mathbf{x}^+)$ stands for the evaluation of \bullet on the positive side of the interface (pointed by the normal vector) and $\bullet(\mathbf{x}^-)$ for the evaluation of \bullet on the negative side. As stated in [10, 11, 12], the Nitsche approach can be viewed as a stabilized Lagrange multiplier approach (with condensed multiplier), and parameter β plays role as stabilization parameter and ensures the coercivity of the modified bilinear form. In practice the value of β is approximated by means of an eigenvalue problem proposed by Griebel et al. [13].

3 NUMERICAL EXAMPLES

In the proposed approach, the geometrical approximation of the interfaces is maintained linear although the order of the approximation is increased. It is well known that high-order approximations are very sensitive to the geometrical accuracy. However, as proved in [14], optimal convergence can still be obtained provided that the size of the geometrical grid h_g verified the following estimate:

$$h_g = \alpha h^{2p/3} \quad (2)$$

Where h is the size of the approximation mesh and p is the order of the approximation.

3.1 Material interfaces

The convergence of this approach in conjunction with Nitsche is now studied. Consider an infinite plate subjected to equibiaxial tension and containing a circular inclusion of radius $a = 0.4$ mm at its center. The approximation domain consists in a square of length 2.0 mm centered on point $(0, 0)$. The two materials are considered as linear elastic with Young's modulus $E_m = 1.0$ MPa and Poisson's ratio $\nu_m = 0.3$ for the matrix. Concerning the inclusion, the following parameters are considered: $E_i = 10.0$ MPa and $\nu_i = 0.25$. The analytical solution of this problem was given in [15] and is used to apply exact tractions on the boundary of the approximation domain. Only the case of p convergence is considered here: An approximation mesh composed of 4×4 elements per side, and a geometrical mesh with refined elements along the interface are considered. Four geometrical meshes are considered depending on the size of the elements near the interface (size 2^{-4} , 2^{-5} , 2^{-7} and 2^{-9}). In all the cases, the value of Nitsche's parameter is obtained by solving the eigenvalue problem associated to the stability condition. The results are depicted in figure 2. One can see that an exponential convergence can be obtained during p refinement provided that the geometrical accuracy is sufficient. When it is no more the case, the convergence slows down, then stops at a level that depends on the geometrical accuracy. This behavior is partially linked to the contrast between the inclusion and the matrix. A comparison between contrast 10 and 100 is presented in figure 2 (with the same geometrical accuracy of level 10). It can be seen that the contrast has a limited influence on the range of optimal convergence, which means that estimate (2) is hardly influenced by the contrast (at least, in this case). On the contrary, the level of the plateau is significantly influenced by the contrast level.

3.2 Mechanical parts

The approach is now illustrated in the case of the static behavior of a mechanical part. In this case, the approach is more related to the Finite Cell approach [1], but with a better representation of the interface. Consider the example depicted in figure 3(a) inspired from the one proposed in

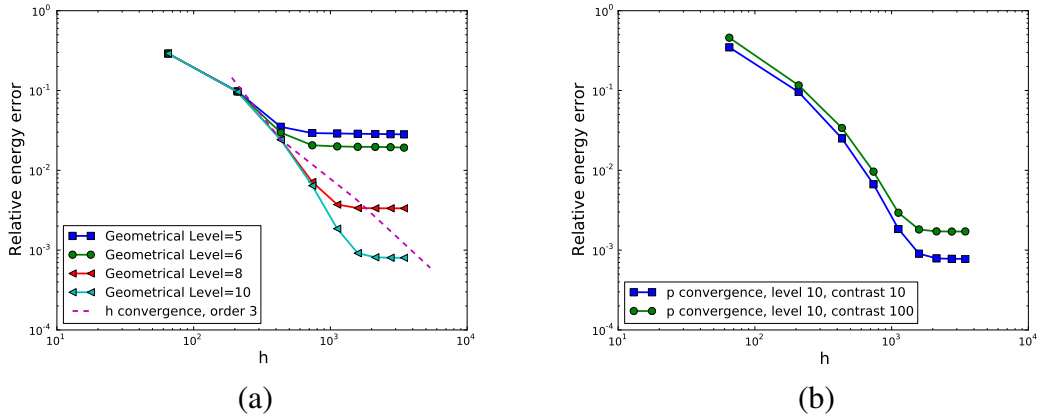


Figure 2: Case of material interfaces: p Convergence with respect to the number of dofs. (a) influence of the geometrical accuracy; (b) influence of the contrast. (Note that the geometrical description of the cubic h convergence was obtained following [14])

[16] which represents a flywheel subjected to a torsional loading. The geometry of the flywheel is represented with a levelset that is interpolated on a level 9 octree mesh (512 elements per side) whose bounding box is 40% larger than the part's bounding box. The approximation mesh consists in a regular level 4 mesh (16 elements per side) (see figure 3(b)), but an adapted octree could also be considered with the use of a proper error estimator. The geometrical mesh is presented in figure 4(a), and the resulting integration cells in figure 4(b). The results are depicted in figure 5 for degree 4 and 7 X-FEM approximations (resp 4434 and 12 978 dofs) and a conforming FEM degree 4 approximation (128 704 dofs, sub-parametric linear mesh). One can see that the stress distribution is consistent between FEM and X-FEM computations with much less degrees of freedom. If now the strain energy of the flywheel is computed, it can be seen that degree 4 X-FEM approximation leads to a 3.59% discrepancy for 3.45% of the dofs of the reference solution. Concerning the degree 7 X-FEM approximation, a 0.44% error is obtained with 10.1% of the dofs of the reference solution (see table 1).

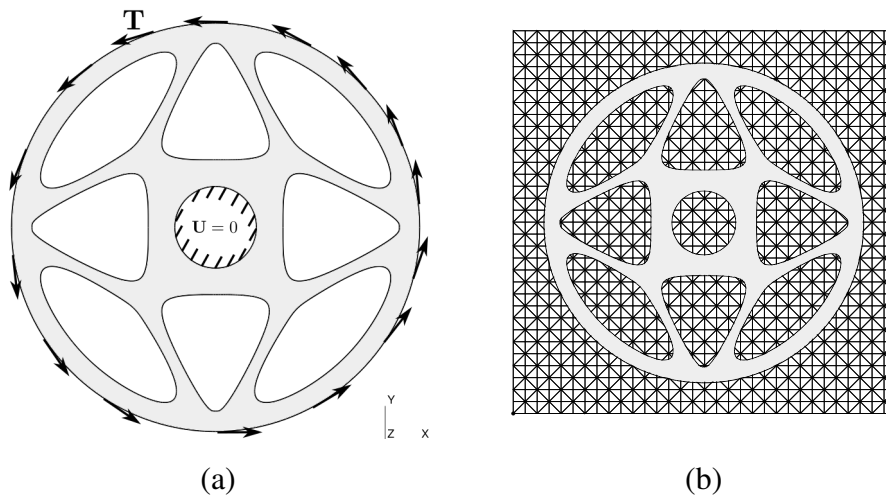


Figure 3: Flywheel subjected to a torsional loading: (a) Geometry and boundary conditions; (b) Approximation mesh.

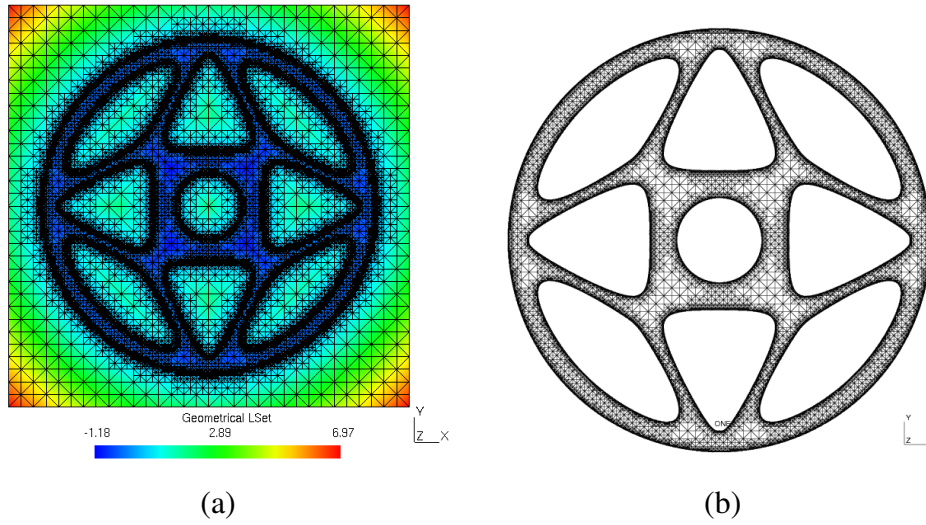


Figure 4: Flywheel subjected to a torsional loading: (a) Levelset on the geometrical octree; (b) Integration cells in the domain.

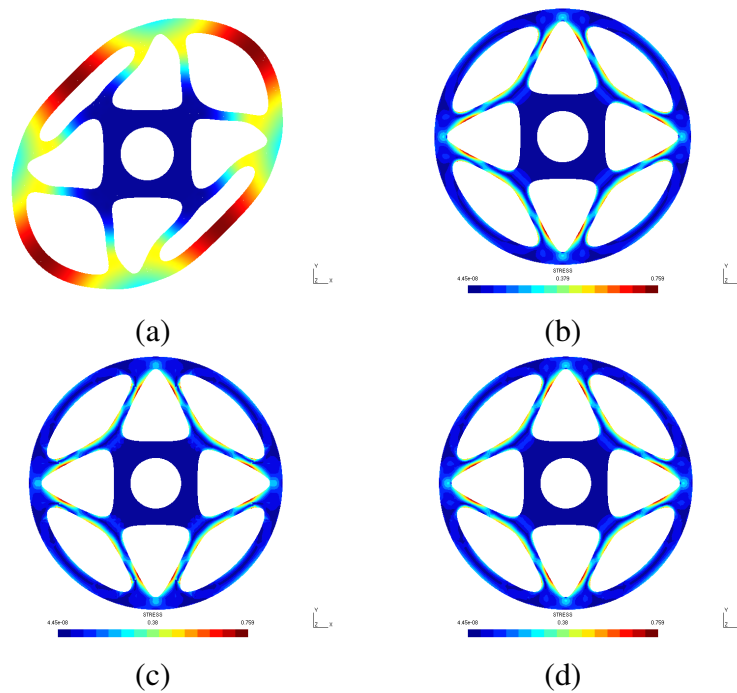


Figure 5: Flywheel subjected to a torsional loading: (a) Displacement, $p = 4$ FEM approximation (64 352 dofs); (b) Von Mises stress, $p = 4$ FEM approximation; (c) Von Mises stress, $p = 4$ X-FEM approximation (4434 dofs) and (d) Von Mises stress, $p = 7$ X-FEM approximation (12 978 dofs)

Case	Nb Dofs (Ratio/Fem)	Error/Fem
Fem	128704 (1.0)	Ref.
X-FEM $p = 4$	4434 (0.034451)	3.5937 %
X-FEM $p = 7$	12978 (0.10084)	0.44273 %

Table 1: Flywheel subjected to a torsional loading: Comparison between Fem and X-FEM

4 CONCLUSION

A computational approach is proposed for the treatment of image-based computations. It allows to uncouple the geometrical resolution from the approximation mesh. It was shown that optimal convergence rates could be obtained in the case of material interfaces, and that the approach can be more efficient than classical FEM in the case of level-set based geometries. More validations about the current approach, and its application to real image-based computations are presented in [17]. This approach could be combined to the strategy proposed in [18] for the treatment of complex real CAD geometries.

REFERENCES

- [1] Jamshid Parvizian, Alexander Duster, and Ernst Rank. Finite cell method - h and p extension for embedded domain problems in solid mechanics. *Computational Mechanics*, 41(1):121–133, 2007.
- [2] T. Strouboulis, L. Zhang, and I. Babuška. p-version of the generalized fem using mesh-based handbooks with applications to multiscale problems. *International Journal for Numerical Methods in Engineering*, 60(10):1639–1672, 2004.
- [3] J. P. Pereira, C. A. Duarte, D. Guoy, and X. Jiao. hp -Generalized FEM and crack surface representation for non-planar 3-D cracks. *International Journal for Numerical Methods in Engineering*, 77(5):601–633, 2009.
- [4] A. Legay, H.W. Wang, and T. Belytschko. Strong and weak arbitrary discontinuities in spectral finite elements. *International Journal for Numerical Methods in Engineering*, 64:991–1008, 2005.
- [5] Kwok Wah Cheng and Thomas-Peter Fries. Higher-order XFEM for curved strong and weak discontinuities. *International Journal for Numerical Methods in Engineering*, 82:564590, 2009.
- [6] Kristell Dréau, Nicolas Chevaugeon, and Nicolas Moës. Studied X-FEM enrichment to handle material interfaces with higher order finite element. *Computer Methods in Applied Mechanics and Engineering*, 199(29-32):1922–1936, 2010.
- [7] T. Strouboulis, I. Babuška, and K. Copps. The design and analysis of the generalized finite element method. *Computer Methods in Applied Mechanics and Engineering*, 181:43–69, 2000.
- [8] G. Legrain, P. Cartraud, Perreard I., and N. Moës. An x-fem and level set computational approach for image-based modelling: Application to homogenization. *International Journal for Numerical Methods in Engineering*, 86(7):915934, 2011.

- [9] E. Budyn, G. Zi, N. Moës, and T. Belytschko. A method for multiple crack growth in brittle materials without remeshing. *International journal for numerical methods in engineering*, 61:1741–1770, 2004.
- [10] Anita Hansbo and Peter Hansbo. A finite element method for the simulation of strong and weak discontinuities in solid mechanics. *Computer Methods in Applied Mechanics and Engineering*, 193(33-35):3523–3540, August 2004.
- [11] Rolf Stenberg. On some techniques for approximating boundary conditions in the finite element method. *Journal of Computational and Applied Mathematics*, 63(1-3):139–148, November 1995.
- [12] Anand Embar, John Dolbow, and Isaac Harari. Imposing dirichlet boundary conditions with nitsche’s method and spline-based finite elements. *International Journal for Numerical Methods in Engineering*, 83:877–898, 2010.
- [13] M. Griebel and M.A. Schweitzer. *Geometric Analysis and Nonlinear Partial Differential Equations*, chapter A particle-partition of unity method. Part V: Boundary conditions, pages 517 – 540. Springer-Verlag, Berlin, 2002.
- [14] A. Huerta, E. Casoni, E. Sala-Lardies, S. Fernandez-Mendez, and J. Peraire. Modeling discontinuities with high-order elements. In *ECCM 2010 - Paris*, 2010.
- [15] N. Sukumar, D. L. Chopp, N. Moës, and T. Belytschko. Modeling Holes and Inclusions by Level Sets in the Extended Finite Element Method. *Comp. Meth. in Applied Mech. and Engrg.*, 190:6183–6200, 2001.
- [16] J. J. Ródenas-garcía, E. Nadal, J. Albelda, and F. J. Fuenmayor Fernández. H-adaptive refinement based on a nearly statically admissible recovered stress field for meshes independent of the geometry. In *IV European Conference on Computational Mechanics*, 2010.
- [17] G. Legrain, N. Chevaugéon, and K. Dréau. High order x-fem and levelsets for complex microstructures: Uncoupling geometry and approximation. *Computer Methods in Applied Mechanics and Engineering*, n/a:Accepted, 2012.
- [18] Mohammed Moumnassi, Salim Belouettar, ric Bchet, Stphane P.A. Bordas, Didier Quoirin, and Michel Potier-Ferry. Finite element analysis on implicitly defined domains: An accurate representation based on arbitrary parametric surfaces. *Computer Methods in Applied Mechanics and Engineering*, 200(5-8):774 – 796, 2011.